

Evaluation of Weather Parameters for Renewable Energy Forecasting with Echo State Networks

Samuel G. Dotson^{a,*}, Kathryn D. Huff^a

^a*Dept. of Nuclear, Plasma, and Radiological Engineering, University of Illinois at Urbana-Champaign, Urbana, IL 61801*

Abstract

The abstract goes here. As a general guide, you should provide a concise (150-250 words) summary of your article - introduction, methodology, results, and conclusion. Avoid using abbreviations and acronyms unless the abbreviation/acronym is used repeatedly in the abstract. There should be no references in the abstract.

Keywords: FIXME, key words, go here, like:, simulation, spent nuclear fuel

1. Introduction

1.1. Motivation

Reducing carbon emissions has become a priority for many countries in response to the rising threat of climate change. The goal set by the 2015 Paris Agreement is to prevent the global temperature from rising more than 1.5 °C above pre-industrial levels [1]. Virtually all current plans to reduce carbon emissions depend on increasing the share of energy production by renewable and clean energy sources, especially solar and wind energy [2, 3, 4, 5]. While solar and wind are low-carbon sources, these forms of electricity generation are variable and unpredictable. This variability is found to be major cause of blackouts and power system failures [6]. Further, even modest penetrations of renewable energy negatively affect the economics of other types of clean energy, such as nuclear power [2, 7, 8]. This may force nuclear plants to shutdown prematurely, at the precise moment clean sources of energy are most needed. There has been some work done to quantify the economic benefit of improving forecasts of renewable energy [9, 10, 11]. Some of the benefits of improving forecasts are: 1) It is often cheaper than building storage devices [9]. 2) Would reduce curtailment and allow for efficient use of non-renewable sources [10]. 3) Enable a slight, but important, amount of

load-following from nuclear and bio-mass generators which are not designed for rapid load following [11]. Most proposed forecasting improvements involve new algorithms or machine learning techniques. However, one of the simplest approaches to improving forecasts is to improve the training data for such algorithms. There is a veritable zoo of weather parameters that can supplement target training data and we don't know *a priori* which of these parameters will be helpful or detrimental to model performance. In this paper, we evaluate several common parameters for use in renewable energy forecasting with Echo State Networks (ESNs).

1.2. Why Echo State Networks

ESNs have several appealing features. They are simple, consisting only of a large sparse reservoir and a single output layer [12]; flexible and generalizable where other network architectures require significant fine tuning [13]; and fast, due to their simple structure and very few trainable weights relative to other neural networks. Additionally, ESNs have been shown to outperform other prediction techniques [14, 15, 16, 17, 18].

Classical ESNs have previously been used to forecast demand, wind energy, and solar energy [19, 15, 18]. ESNs are typically used to make very short term predictions, on the order of seconds or minutes [20, 21, 17], one-hour ahead [16], up to a single day ahead [19]. Forecasts need to be multiple-hours to a couple of days ahead to aid unit commitment and grid-scale energy economy [9, 10, 11].

*Corresponding Author

Email address: sgd2@illinois.edu (Samuel G. Dotson)

In this work we use a classic ESN architecture to
60 forecast total demand, wind production, and solar production, 4-hours and 48-hours ahead.

There has been a lot of work to improve the forecasting capability of the basic ESN. Approaches include adding multiple reservoirs [18, 22, 23, 24];
65 including non-linear units [25, 17]; combining with other network architecture [20, 26]; and using a particle swarm approach [27, 21]. Some works mention that including weather parameters may be useful for renewable energy forecasting [28, 17] but none
70 have demonstrated the effect each parameter has on model performance. The primary goal of this work is to fill that gap.

1.3. Contributions

In this work, we use ESNs for three main prediction tasks: Total electricity demand, wind energy production, and solar energy production. We split these tasks into further sub tasks; predicting four hours ahead, and 48- hours ahead. These predictions are useful for scheduling and grid planning because
75 current market rules put renewable energy on the grid first, forcing conventional power generators to work around this variability [9]. Using ESNs to make predictions two-days ahead is unique this paper since the longest predictions by ESNs in the literature is only one-day ahead [19]. Finally, we repeat these
80 tasks with several commonly used weather parameters and evaluate their effect on model performance. The need to consider exogenous meteorological inputs has been noted previously. Surprisingly, using sun elevation as a correlated quantity for energy demand and wind power is absent from the literature.
85

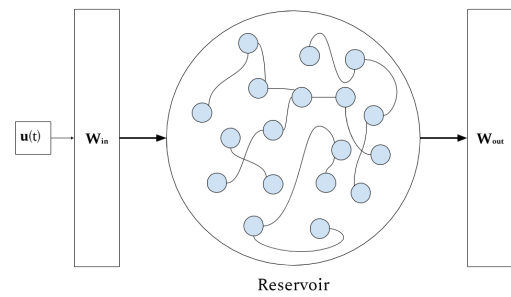
The structure of the paper is as follows. In section 2, we discuss how data was selected, processed, and review ESNs. Section 3 shows a benchmarking
90 exercise for our ESN implementation and presents the results. We discuss the results and future implications in section 4.

2. Methodology

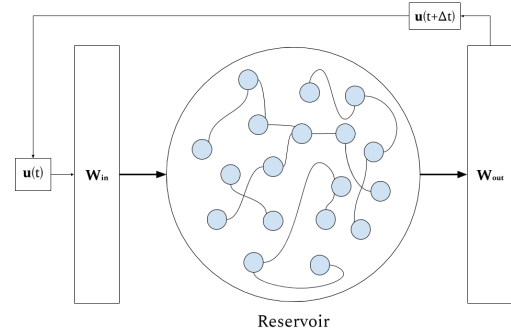
2.1. Echo State Networks

An ESN, sometimes called a “reservoir computer,”[29, 30, 31] is a type of recurrent neural network that replaces the many hidden layers of a conventional feed- forward neural network with a reservoir that is
100

105 1. sparse.



(a) Training Flow



(b) Predicting Flow

Figure 1: Reservoir behavior in the training and predicting phases.

2. connected by uniformly random weights, centered at zero.
3. large (i.e. has many neurons).

The reservoir is therefore a randomly instantiated adjacency matrix, \mathbf{W} , of size $N \times N$. The input vector, $U(t)$, of K units is mapped onto the reservoir by an input matrix, W^{in} of size $N \times K$. The activation states of the reservoir are calculated by

$$x(t) = \tanh(W^{in} \cdot U(t) + \mathbf{W}x(t-1)) \quad (1)$$

Where $x(t)$ is the collection of reservoir activations [16, 30, 12]. The output is read by an output weight matrix, W^{out} .

$$U(t + \Delta t) = (W^{out})^T \cdot x(t) \quad (2)$$

In the training phase, the output, $U(t + \Delta t)$, is discarded and the next training input passed to the network. During the prediction phase, the output is kept and used as the next input. This behavior is shown in Figure 1. The speed of ESNs is owed to this structure; only W^{out} has tunable weights.

Everything else is fixed. In this work, we adapted the open source Python package pyESN [32] to construct and train the network.

2.2. Hyper-parameter Optimization

ESNs are fast because the hidden layer in a conventional feed-forward neural network is replaced by a large reservoir that does not require training. The trade off is that ESNs are sensitive to various hyper-parameters that need to be optimized [12]. These hyper-parameters are summarized in Table 1. The spectral radius (ρ) should satisfy the “echo state property” which means that previous reservoir activations have a decaying influence on future states. This is usually guaranteed for $\rho < 1$, but is not a requirement [12].

The hyper-parameters are optimized by performing a grid search over the test values specified in Table 1. The following steps were taken for each prediction task:

1. Select a hyper-parameter or pair of parameters.
2. Generate ESN prediction with the specified parameters.
3. Calculate and record the RMSE.
4. Continue until last entry in the parameter set is reached.
5. Set the network parameters to hyper-parameter value that minimizes the RMSE.

This algorithm generates an error surface where the coordinates of the absolute minimum correspond to the indices of values in the hyper-parameter test sets that minimized the RMSE.

2.3. Prediction Tasks

We first performed a benchmarking task by making a prediction for the Lorenz 1963 model [33]. Then we optimized predictions for univariate time-series representing total demand, solar energy, and wind energy 4-hours ahead and 48- hours ahead. Finally, those same six tasks are repeated with an additional predictor. The tasks are summarized in Table 2.

2.4. Data Selection and Processing

All data predicting demand, wind energy, and solar energy on the University of Illinois at Urbana-Champaign (UIUC) campus are from the UIUC Solar Farm 1.0 dashboard [34] and proprietary data shared with us courtesy of the UIUC Facilities and Services Department. All data had hourly resolution. Weather data was retrieved from the National Oceanic and Atmospheric Administration (NOAA)[35] for two locations: Champaign, IL, where UIUC is located, and Lincoln, IL, where Rail-splitter Windfarm is located. UIUC has a power purchase agreement with Rail-splitter Windfarm [36]. In the case of UIUC solar data, significant portions were missing due to instrument failure. In order to fill in this missing data, we calculated the theoretical solar energy production based on irradiance data from OpenEI [37]. The solar output is given by [38]

$$P = G_T \eta_{ref} \tau_{pv} A [1 - \gamma(T - 25)] [W] \quad (3)$$

where

$$\begin{aligned} G_T &= P_{DNI} * \cos(\beta + \delta - lat) \\ &+ P_{DHI} * \left(\frac{180 - \beta}{180} \right) \left[\frac{W}{m^2} \right] \end{aligned} \quad (4)$$

where

$$\delta = 23.44 \sin \left(\left(\frac{\pi}{180} \right) \left(\frac{360}{365} \right) (N + 284) \right) [\text{degrees}] \quad (5)$$

η, τ, γ are solar panel properties

P_{DNI} is the direct normal irradiance

P_{DHI} is the diffuse horizontal irradiance

β is the tilt angle of the solar panels

Table 1: Description of Model Hyper-parameters

Hyper-parameter	Purpose	Tested Values
noise	Neuron regularization	[0.0001, 0.0003, 0.0007, 0.001, 0.003, 0.005, 0.007, 0.01]
ρ	Spectral radius	[0.5, 0.7, 0.9, 1, 1.1, 1.2, 1.3, 1.5]
N	Size of reservoir, \mathbf{W}	[600, 800, 1000, 1500, 2000, 2500, 3000, 4000]
sparsity	The density of connections in \mathbf{W}	[0.005, 0.01, 0.03, 0.05, 0.1, 0.12, 0.15, 0.2]
Training Length	Size of the training set before prediction	$L \in [5000, 25000]$, step size = 300

Table 2: Summary of Prediction Tasks

Target	Future	Additional Predictor
Total Demand	4 hours ahead	None Solar Elevation
Solar Energy	48 hours ahead	Humidity Pressure
Wind Energy		Wet Bulb Temp. Dry Bulb Temp. Wind Speed

The solar elevation angle, α , was also calculated [39, 40] using coordinates for the UIUC solar farm.

$$\alpha = \sin^{-1} [\sin(\delta) \sin(\phi) + \cos(\delta) \cos(\phi) \cos(\omega)] \quad (6)$$

where

δ is the declination angle

ϕ is the latitude of interest

ω is the hour angle

Finally, we normalized all of the data using the infinity norm

$$\|\mathbf{x}\|_\infty \equiv \max |x_i|. \quad (7)$$

The infinity norm is equivalent to normalizing by the system capacity. This is useful because it simplifies the comparison of our results between tasks whose training data have vastly different magnitudes.

2.5. Error Metric

We measure the accuracy of the model using two error metrics: Mean absolute error (MAE) and root

mean squared error (RMSE). These are defined as

$$\text{MAE} = \frac{1}{N} \sum_{i=1}^N |y_i - \hat{y}_i| \quad (8)$$

$$\text{RMSE} = \sqrt{\frac{1}{N} \sum_{i=1}^N (y_i - \hat{y}_i)^2} \quad (9)$$

The MAE measures the expected error throughout the forecast horizon. The RMSE indicates the presence of large but infrequent errors. Since the data were normalized by system capacity [9], the error metrics are easily interpretable.

3. Results

Below we show the best prediction for each task.

3.1. Benchmark: Lorenz 1963

We first verified that our choice of implementation for ESNs produces similar results to those found in the literature [29]. The hyper-parameters that minimized the RMSE of the model can be found in Table 3. Our optimized values are somewhat different from the literature, but our ESN implementation successfully replicated the climate of the Lorenz Attractor similar to Pathak et. al 2017.

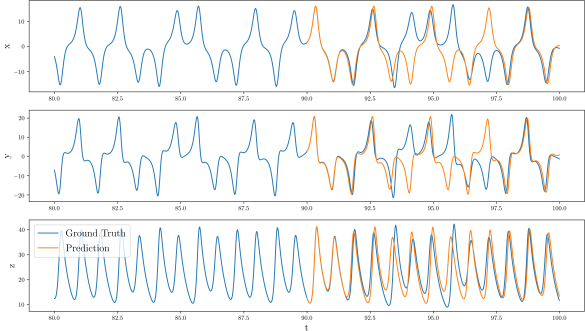


Figure 2: Using an ESN to replicate the climate of the Lorenz Attractor.

Table 3: Hyper-parameters for the Lorenz 1963 Model

Parameter	This paper	Literature [29]
N	2000	300
ρ	0.9	1.2
sparsity	0.1	0.1
noise	0.001	0
Training Length	3200	Not Specified

4. Discussion

The forecast accuracy of our ESN for the Lorenz model does not persist for quite as long as in other works [29]. However, our model successfully replicates the environment that produces the Lorenz Attractor. Further, optimal parameters may be unique for each randomly instantiated reservoir. It is impossible to replicate the exact conditions of other works without information about a seed for the random state. We have included this information for future work to compare with our results.

For each target variable, demand, wind, and solar, we found that air pressure was the only meteorological factor that improved the forecast error in every case. Solar elevation angle also decreased the error in most cases with one exception, 48-hour ahead solar production. One possible reason for the improved performance from adding air pressure is that the data may contain implicit information about weather dynamics. For example, air pressure typically changes throughout the day due to solar heating and has close relationship to air temperature [41], thus it contains implicit information about both the amount of solar energy reaching the ground and the ambient temperature which influences electricity demand and solar energy generation. Similarly, the height of the sun in the sky has a strong influence on ambient weather and thus on demand

and the production of renewable energy. Elevation angle lacks information about how much solar energy reaches the ground, which could explain why air pressure performed better in some cases. Using the solar angle to improve forecasting has a couple of important advantages over measured weather data. First, it can be calculated accurately within a minute time-resolution [39]. Second, because solar angle can be calculated deterministically, it reduces the amount of data processing required. Based on this, we recommend using solar elevation as a simple first attempt at improving forecasts.

The results also show that some meteorological factors are detrimental to model performance. In particular, Table ?? and 4 show that temperature increased both the MAE and RMSE for the model. This is counter to conventional wisdom that air temperature influences electricity demand. Additionally, we recommend that researchers forecast demand, solar, and wind energy separately, rather than packaged together as a net demand, because they each possess unique and potentially interfering dynamics.

The forecast lengths were decided based on the requirements for improved economics and planning mentioned in the literature [9, 10, 11]. The ESN model performed reasonably well at predicting four hours ahead but is not an improvement over the state-of-the-art [9, 42]. The model did not perform well at the 48-hour ahead forecasts. This could be due to the lack of higher resolution data. ESNs are known for their ability to predict highly non-linear systems [43, 44] yet using hourly data could add superfluous complexity that confounds the model [45]

4.1. Future Work

One appealing avenue of continued work is to leverage ESNs to generate synthetic data that respects real dynamics. Synthetic data is often useful for other machine learning or optimization algorithms. Typically, these data are produced by sampling from an Auto-regressive Moving Average (ARMA) model [46, 47], which tacitly assumes the training data can be made stationary. ESNs have been shown to replicate the environment of a dynamical system, although it remains to be seen how far in the future this behavior persists [29, 30]. Future work will also explore the effect of data resolution on model performance, as well as evaluate some of the improvements to the ESN algorithm.

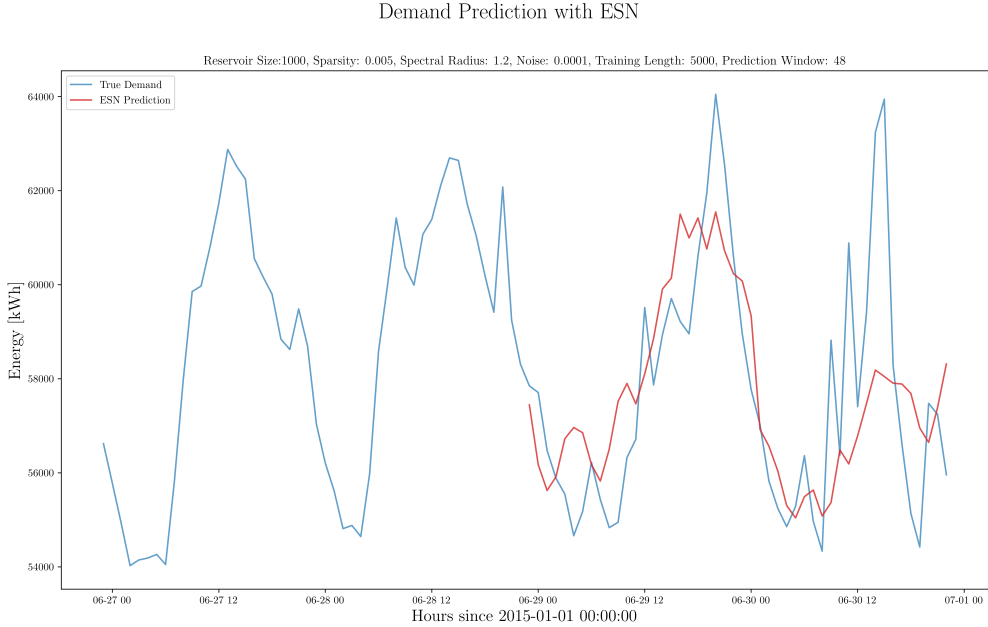


Figure 3: The optimized 48-hour ahead demand prediction with pressure as a meteorological predictor.

Table 4: Tabulated error for 48-hour ahead total electricity demand forecasts with various coupled quantities. Improvement indicates the percentage improvement over the base case of forecasting electricity demand alone.

Scenario	MAE	RMSE	Improvement MAE (%)	Improvement RMSE (%)
Total Demand	0.018892	0.024137	[-]	[-]
Demand + Sun Elevation	0.013375	0.022893	-29.20	-5.15
Demand + Humidity	0.048357	0.063544	+155.96	+163.26
Demand + Pressure	0.009329	0.017334	-50.62	-28.18
Demand + Wet Bulb Temp.	0.033473	0.039922	+77.18	+65.40
Demand + Dry Bulb Temp.	0.031866	0.040409	+66.67	+67.42
Demand + Wind Speed	0.051045	0.074966	+170.19	+210.58

Table 5: Tabulated error for 4-hour ahead electricity demand forecasts with various coupled quantities. Improvement indicates the percentage improvement over the base case of forecasting solar energy alone.

Scenario	MAE	RMSE	Improvement MAE (%)	Improvement RMSE (%)
Total Demand	0.019343	0.026322	[-]	[-]
Demand + Sun Elevation	0.009869	0.016928	-48.98	-35.69
Demand + Humidity	0.054772	0.073056	+183.16	+177.54
Demand + Pressure	0.009754	0.019314	-49.57	-26.62
Demand + Wet Bulb Temp.	0.020932	0.026979	+8.21	+2.50
Demand + Dry Bulb Temp.	0.026577	0.039963	+37.40	+51.82
Demand + Wind Speed	0.042534	0.067427	+119.89	+156.16

255 5. Conclusion

Improving renewable energy forecasting is impor- 260 tant for grid-planning and unit commitment. Espe-

cially as the share of variable renewable resources increases, challenging the baseload power from nuclear plants. We first demonstrated that our im-

Demand Prediction with ESN

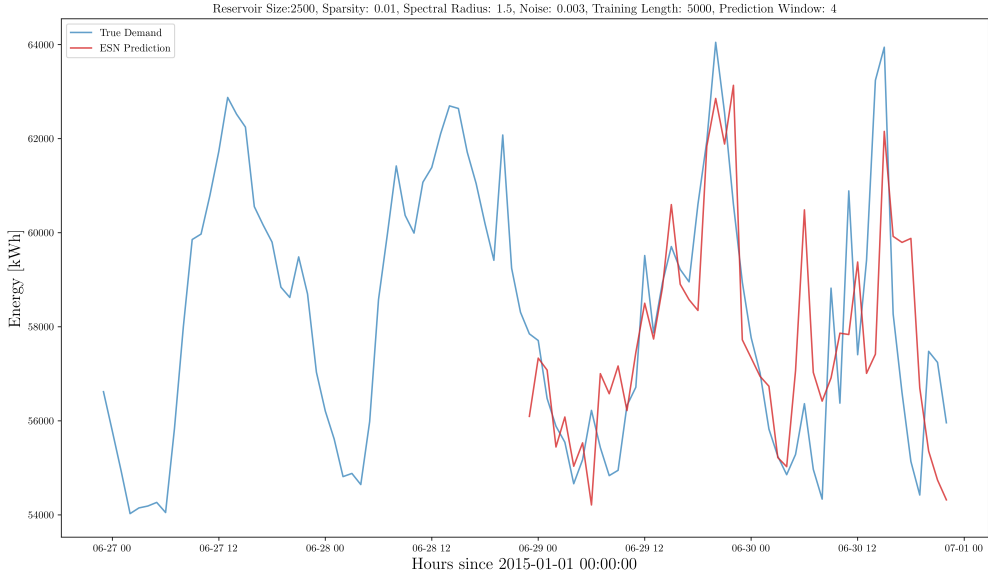


Figure 4: The optimized 4 hour ahead demand prediction with solar angle as an additional predictor.

Solar Generation Prediction with ESN

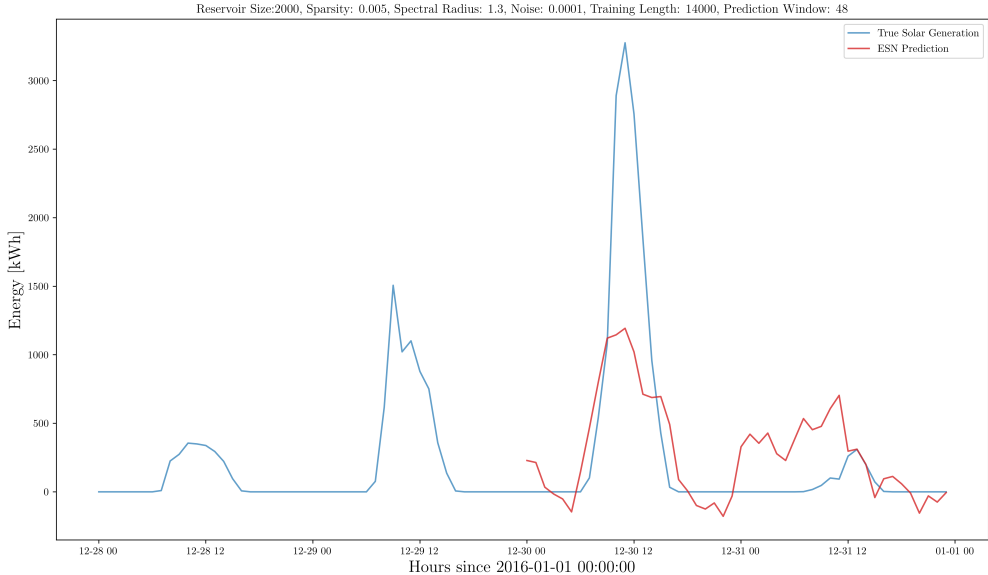


Figure 5: The optimized 48-hour ahead solar energy prediction with humidity as a meteorological predictor.

lementation of the ESN algorithm is consistent with the literature. Then we applied this model to prediction tasks for total demand, solar energy, and wind energy, and evaluated the influence of several meteorological factors on model performance. Our results show that only air pressure and solar

angle were consistently good at improving model accuracy. However, the conventional ESN used here did not demonstrate a significant improvement over the state-of-the-art. Nor was it accurate enough to improve grid-scale energy economy. Future work will explore other applications of ESNs and evaluate

Table 6: Tabulated error for 48-hour ahead solar energy forecasts with various coupled quantities. Improvement indicates the percentage improvement over the base case of forecasting solar energy alone.

Scenario	MAE	RMSE	Improvement MAE (%)	Improvement RMSE (%)
Solar Energy	0.143276	0.206162	[−]	[−]
Solar + Sun Elevation	0.200627	0.292516	+40.02	+41.88
Solar + Humidity	0.086920	0.111476	-39.33	-45.93
Solar + Pressure	0.098554	0.152672	-31.21	-25.94
Solar + Wet Bulb Temp.	0.114157	0.167503	-20.32	-18.75
Solar + Dry Bulb Temp.	0.079036	0.123783	-44.84	-39.96
Solar + Wind Speed	0.147270	0.191722	+2.788	-7.004

Solar Generation Prediction with ESN

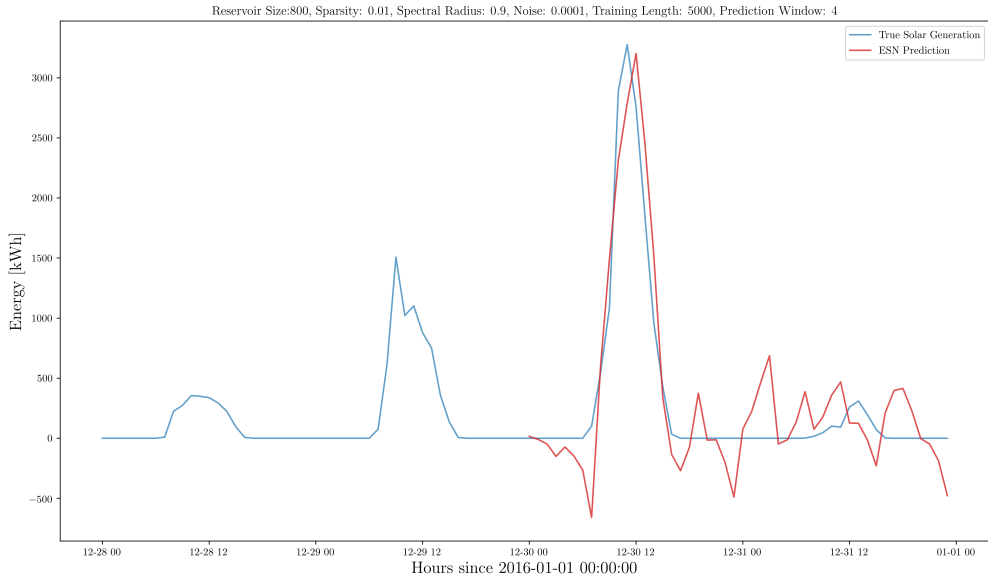


Figure 6: The optimized 4 hour ahead solar energy prediction with wet bulb temperature as a meteorological predictor.

Table 7: Tabulated error for 4-hour ahead solar energy forecasts with various coupled quantities. Improvement indicates the percentage improvement over the base case of forecasting solar energy alone.

Scenario	MAE	RMSE	Improvement MAE (%)	Improvement RMSE (%)
Solar Energy	0.061426	0.095794	[−]	[−]
Solar + Sun Elevation	0.033263	0.060048	-45.85	-37.32
Solar + Humidity	0.054951	0.078739	-10.54	-17.80
Solar + Pressure	0.046862	0.089294	-23.71	-6.78
Solar + Wet Bulb Temp.	0.038104	0.053419	-37.97	-44.24
Solar + Dry Bulb Temp.	0.044104	0.073112	-28.20	-23.68
Solar + Wind Speed	0.070293	0.099912	+14.44	+4.30

improvements to the model algorithm.

6. Acknowledgments

275 This work was made possible with the support from the people at UIUC Facilities & Services. In

Wind Generation Prediction with ESN

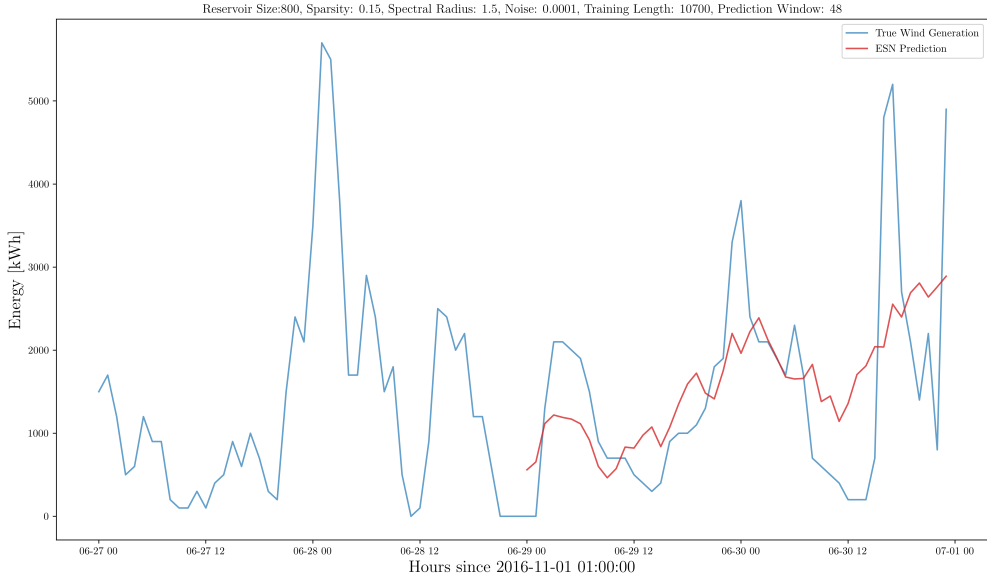


Figure 7: The optimized 48-hour ahead wind energy prediction with solar angle as an additional predictor.

Table 8: Tabulated error for 48-hour ahead wind forecasts with various coupled quantities. Improvement indicates the percentage improvement over the base case of forecasting wind energy alone.

Scenario	MAE	RMSE	Improvement MAE (%)	Improvement RMSE (%)
Wind Energy	0.103516	0.130848	[-]	[-]
Wind + Sun Elevation	0.051899	0.081339	-49.82	-37.84
Wind + Humidity	0.091975	0.112054	-11.15	-14.36
Wind + Pressure	0.054388	0.097670	-47.46	-25.36
Wind + Wet Bulb Temp.	0.074085	0.097004	-28.43	-25.86
Wind + Dry Bulb Temp.	0.081268	0.105289	-21.49	-19.53
Wind + Wind Speed	0.100880	0.122271	-2.5464	-6.555

Table 9: Tabulated error for 4-hour ahead wind forecasts with various coupled quantities. Improvement indicates the percentage improvement over the base case of forecasting wind energy alone.

Scenario	MAE	RMSE	Improvement MAE (%)	Improvement RMSE (%)
Wind Energy	0.090266	0.124303	[-]	[-]
Wind + Sun Elevation	0.039248	0.083134	-56.52	-33.12
Wind + Humidity	0.064131	0.096310	-28.95	-22.52
Wind + Pressure	0.043739	0.087981	-51.54	-29.22
Wind + Wet Bulb Temp.	0.044447	0.077770	-50.76	-37.44
Wind + Dry Bulb Temp.	0.050536	0.083151	-44.01	-33.11
Wind + Wind Speed	0.063456	0.088157	-29.70	-29.07

particular, Morgan White, Mike Marquissee, and Mike Larson. It was also aided by other members of the Advanced Reactors and Fuel Cycles (ARFC)

group, in particular Nathan Ryan. This work is supported by the Nuclear Regulatory Commission Fellowship Program. Prof. Huff is supported by

Wind Generation Prediction with ESN

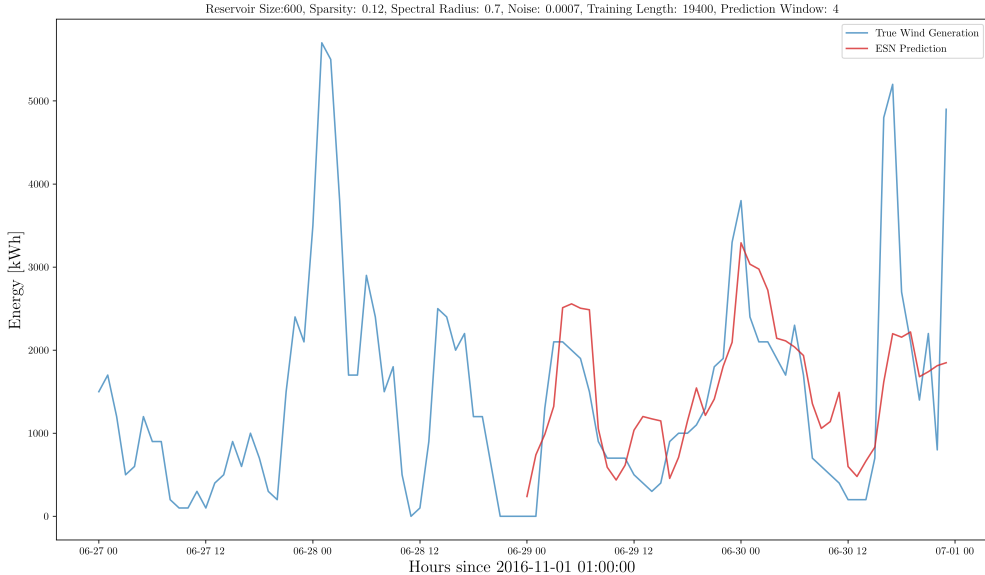


Figure 8: The optimized 4 hour ahead wind energy prediction with wet bulb temperature as a meteorological predictor.

the Nuclear Regulatory Commission Faculty Development Program (award NRC-HQ-84-14-G-0054 285 Program B), the Blue Waters sustained-petascale computing project supported by the National Science Foundation (awards OCI-0725070 and ACI-1238993) and the state of Illinois, the DOE ARPA-E MEITNER Program (award DE-AR0000983), and the DOE H2@Scale Program (Award Number: DE-EE0008832)

References

- [1] The paris agreement | UNFCCC.
URL <https://unfccc.int/process-and-meetings/the-paris-agreement/the-paris-agreement>
- [2] C. Cany, C. Mansilla, G. Mathonnière, P. da Costa, Nuclear contribution to the penetration of variable renewable energy sources in a french decarbonised power mix 150 544–555. doi:[10.1016/j.energy.2018.02.122](https://doi.org/10.1016/j.energy.2018.02.122).
URL <http://www.sciencedirect.com/science/article/pii/S0360544218303566>
- [3] J. Chilvers, T. J. Foxon, S. Galloway, G. P. Hammond, D. Infield, M. Leach, P. J. Pearson, N. Strachan, G. Strbac, M. Thomson, Realising transition pathways for a more electric, low-carbon energy system in the united kingdom: Challenges, insights and opportunities 231 (6) 440–477, publisher: IMECE. doi:[10.1177/0957650917695448](https://doi.org/10.1177/0957650917695448).
URL <https://doi.org/10.1177/0957650917695448>
- [4] 99th General Assembly, Illinois general assembly - full text of SB2814.
URL <http://www.ilga.gov/legislation/fulltext.asp?DocName=&SessionId=88&GA=99&DocTypeId=315>
- [5] iSEE, Illinois climate action plan (iCAP). URL <https://sustainability.illinois.edu/campus-sustainability/icap>
- [6] H. Haes Alhelou, M. E. Hamedani-Golshan, T. C. Njenda, P. Siano, A survey on power system black-out and cascading events: Research motivations and challenges 12 (4) 682, number: 4 Publisher: Multidisciplinary Digital Publishing Institute. doi:[10.3390/en12040682](https://doi.org/10.3390/en12040682). URL <https://www.mdpi.com/1996-1073/12/4/682>
- [7] J. H. Keppler, C. Marcantonini, O. N. E. Agency, O. for Economic Co-operation {and} Development, Carbon pricing, power markets and the competitiveness of nuclear power, Nuclear development, Nuclear Energy Agency, Organisation for Economic Co-operation and Development.
- [8] Illinois Commerce Commision (ICC), I. P. A. (IPA), I. E. P. A. (IEPA), I. D. of Commerce and Economic Opportunity (IDCEO), Potential nuclear power plant closings in illinois. URL http://www.ilga.gov/reports/special/Report_Potential%20Nuclear%20Power%20Plant%20Closings%20in%20IL.pdf
- [9] Q. Wang, C. B. Martinez-Anido, H. Wu, A. R. Florita, B.-M. Hodge, Quantifying the economic and grid reliability impacts of improved wind power forecasting 7 (4) 1525–1537, conference Name: IEEE Transactions on Sustainable Energy. doi:[10.1109/TSTE.2016.2560628](https://doi.org/10.1109/TSTE.2016.2560628).
- [10] E. V. Mc Garrigle, P. G. Leahy, Quantifying the value of improved wind energy forecasts in a pool-based electricity market 80 517–524. doi:[10.1016/j.renene.2015.02.023](https://doi.org/10.1016/j.renene.2015.02.023). URL <http://www.sciencedirect.com/science/320 asp?DocName=&SessionId=88&GA=99&DocTypeId=340>

- 350 [11] C. Brancucci Martinez-Anido, B. Botor, A. R. Florita, 415
 C. Draxl, S. Lu, H. F. Hamann, B.-M. Hodge, The
 value of day-ahead solar power forecasting improvement
 129 192–203. doi:[10.1016/j.solener.2016.01.049](https://doi.org/10.1016/j.solener.2016.01.049).
 URL <http://www.sciencedirect.com/science/article/pii/S0038092X16000736>
- 355 [12] M. Lukoševičius, A practical guide to applying echo state
 networks, in: G. Montavon, G. B. Orr, K.-R. Müller
 (Eds.), *Neural Networks: Tricks of the Trade: Second
 Edition, Lecture Notes in Computer Science*, Springer,
 pp. 659–686. doi:[10.1007/978-3-642-35289-8_36](https://doi.org/10.1007/978-3-642-35289-8_36).
 URL https://doi.org/10.1007/978-3-642-35289-8_36
- 360 [13] Deterministic wind energy forecasting: A re-
 view of intelligent predictors and auxiliary
 methods 195 328–345, publisher: Pergamon.
 doi:[10.1016/j.enconman.2019.05.020](https://doi.org/10.1016/j.enconman.2019.05.020).
 URL <http://www.sciencedirect.com/science/article/pii/S0196890419305655>
- 365 [14] I. Jayawardene, G. K. Venayagamoorthy, Comparison
 of echo state network and extreme learning machine
 for PV power prediction, in: 2014 IEEE Symposium
 on Computational Intelligence Applications in Smart
 Grid (CIASG), pp. 1–8, ISSN: 2326-7690. doi:[10.1109/CIASG.2014.7011546](https://doi.org/10.1109/CIASG.2014.7011546).
- 370 [15] I. Jayawardene, G. Venayagamoorthy, Comparison of
 adaptive neuro-fuzzy inference systems and echo state
 networks for PV power prediction 53 92–102. doi:[10.1016/j.procs.2015.07.283](https://doi.org/10.1016/j.procs.2015.07.283).
- 375 [16] G. Shi, D. Liu, Q. Wei, Energy consumption prediction
 of office buildings based on echo state networks 216 445
 478–488. doi:[10.1016/j.neucom.2016.08.004](https://doi.org/10.1016/j.neucom.2016.08.004).
 URL <http://www.sciencedirect.com/science/article/pii/S0925231216308219>
- 380 [17] M. A. Chitsazan, M. S. Fadali, A. Tryznadlowski, Wind
 speed and wind direction forecasting using echo state
 network with nonlinear functions 131 879–889, publisher:
 Pergamon. doi:[10.1016/j.renene.2018.07.060](https://doi.org/10.1016/j.renene.2018.07.060).
 URL <http://www.sciencedirect.com/science/article/pii/S0960148118308577>
- 385 [18] H. Hu, L. Wang, S.-X. Lv, Forecasting en- 450
 ergy consumption and wind power generation
 using deep echo state network 154 598–613.
 doi:[10.1016/j.renene.2020.03.042](https://doi.org/10.1016/j.renene.2020.03.042).
 URL <http://www.sciencedirect.com/science/article/pii/S0960148120303645>
- 390 [19] A. Deihimi, H. Showkati, Application of echo state
 networks in short-term electric load forecasting 39 (1)
 327–340. doi:[10.1016/j.energy.2012.01.007](https://doi.org/10.1016/j.energy.2012.01.007).
 URL <https://linkinghub.elsevier.com/retrieve/pii/S0360544212000126>
- 395 [20] Y. Chen, Z. He, Z. Shang, C. Li, L. Li, M. Xu, 455
 A novel combined model based on echo state
 network for multi-step ahead wind speed fore-
 casting: A case study of NREL 179 13–29.
 doi:[10.1016/j.enconman.2018.10.068](https://doi.org/10.1016/j.enconman.2018.10.068).
 URL <https://linkinghub.elsevier.com/retrieve/pii/S0196890418311968>
- 400 [21] H. Wang, Z. Lei, Y. Liu, J. Peng, J. Liu, Echo state
 network based ensemble approach for wind power forecast-
 ing 201 112188. doi:[10.1016/j.enconman.2019.112188](https://doi.org/10.1016/j.enconman.2019.112188).
 URL <http://www.sciencedirect.com/science/article/pii/S019689041931194X>
- 405 [22] C. Gallicchio, A. Micheli, Deep echo state network (Deep- 470
 ESN): A brief surveyarXiv:1712.04323.
 URL <http://arxiv.org/abs/1712.04323>
- [23] X. Yao, Z. Wang, H. Zhang, A novel photovoltaic power
 forecasting model based on echo state network 325
 182–189. doi:[10.1016/j.neucom.2018.10.022](https://doi.org/10.1016/j.neucom.2018.10.022).
 URL <http://www.sciencedirect.com/science/article/pii/S0925231218312104>
- [24] Q. Li, Z. Wu, R. Ling, L. Feng, K. Liu, Multi-reservoir
 echo state computing for solar irradiance prediction:
 A fast yet efficient deep learning approach 95 106481.
 doi:[10.1016/j.asoc.2020.106481](https://doi.org/10.1016/j.asoc.2020.106481).
 URL <https://linkinghub.elsevier.com/retrieve/pii/S1568494620304208>
- [25] G. Holzmann, H. Hauser, Echo state networks with filter
 and a delay&sum readout.
- [26] E. López, C. Valle, H. Allende, E. Gil, H. Madsen,
 Wind power forecasting based on echo state networks
 and long short-term memory 11 (3) 526, number: 3
 Publisher: Multidisciplinary Digital Publishing Institute.
 doi:[10.3390/en11030526](https://doi.org/10.3390/en11030526).
 URL <https://www.mdpi.com/1996-1073/11/3/526>
- [27] N. Chouikhi, B. Ammar, N. Rokbani, A. M. Al-
 imi, PSO-based analysis of echo state network
 parameters for time series forecasting 55 211–225.
 doi:[10.1016/j.asoc.2017.01.049](https://doi.org/10.1016/j.asoc.2017.01.049).
 URL <https://linkinghub.elsevier.com/retrieve/pii/S1568494617300649>
- [28] Q. Li, Z. Wu, R. Ling, M. Tan, Echo state network-
 based spatio-temporal model for solar irradiance
 estimation 158 3808–3813, publisher: Elsevier.
 doi:[10.1016/j.egypro.2019.01.868](https://doi.org/10.1016/j.egypro.2019.01.868).
 URL <http://www.sciencedirect.com/science/article/pii/S1876610219309105>
- [29] J. Pathak, Z. Lu, B. R. Hunt, M. Girvan, E. Ott, Using
 machine learning to replicate chaotic attractors and
 calculate lyapunov exponents from data 27 (12) 121102.
 arXiv:1710.07313, doi:[10.1063/1.5010300](https://doi.org/10.1063/1.5010300).
 URL <http://arxiv.org/abs/1710.07313>
- [30] J. Pathak, B. Hunt, M. Girvan, Z. Lu, E. Ott, Model-free prediction of large spatiotemporally chaotic
 systems from data: A reservoir computing approach 120 (2) 024102, publisher: American Physical Society.
 doi:[10.1103/PhysRevLett.120.024102](https://doi.org/10.1103/PhysRevLett.120.024102).
 URL <https://link.aps.org/doi/10.1103/PhysRevLett.120.024102>
- [31] P. R. Vlachas, J. Pathak, B. R. Hunt, T. P. Sapsis,
 M. Girvan, E. Ott, P. Koumoutsakos, Backprop-
 agation algorithms and reservoir computing in
 recurrent neural networks for the forecasting of
 complex spatiotemporal dynamics 126 191–217.
 doi:[10.1016/j.neunet.2020.02.016](https://doi.org/10.1016/j.neunet.2020.02.016).
 URL <http://www.sciencedirect.com/science/article/pii/S0893608020300708>
- [32] C. Korndörfer, pyESN.
 URL <https://github.com/cknd/pyESN>
- [33] E. N. Lorenz, Deterministic nonperiodic flow 20 (2)
 130–141, publisher: American Meteorological Society
 Section: Journal of the Atmospheric Sciences. doi:
 10.1175/1520-0469(1963)020<0130:DNF>2.0.CO;2.
 URL https://journals.ametsoc.org/view/journals/atsc/20/2/1520-0469_1963_020_0130_dnf_2_0_co_2.xml
- [34] AlsoEnergy, University of illinois solar farm dashboard,
<http://s35695.mini.alsoenergy.com/Dashboard/2a5669735065572f4a424541>
 URL <http://go.illinois.edu/solar>

- [35] N. C. for Environmental Information, Find a station | data tools | climate data online (CDO) | national climatic data center (NCDC).
 URL <https://www.ncdc.noaa.gov/cdo-web/datataools/findstation>
- [36] S. Breitweiser, Wind power: University of illinois at urbana-champaign.
 URL https://www.fs.illinois.edu/docs/default-source/news-docs/newsrelease_windppa-factsheet.pdf?sfvrsn=43aaffea_0
- [37] National solar radiation data base - NSRDB viewer - OpenEI datasets.
 URL <https://openei.org/datasets/dataset/national-solar-radiation-data-base/resource/b2074dd9-36a4-4382-a12f-e6795b578404c>
- [38] H. E. Garcia, J. Chen, J. S. Kim, M. G. McKellar, W. R. Deason, R. B. Vilim, S. M. Bragg-Sitton, R. D. Boardman, Nuclear hybrid energy systems regional studies: West Texas & northeastern Arizona. doi:10.2172/1236837.
 URL <https://www.osti.gov/biblio/1236837-nuclear-hybrid-energy-systems-regional-studies-west-texas-northeastern-arizona>
- [39] US Department of Commerce, ESRL global monitoring laboratory - global radiation and aerosols.
 URL <https://www.esrl.noaa.gov/gmd/grad/solcalc/calcdetails.html>
- [40] J. Meeus, Astronomical Algorithms, 2nd Edition, Willmann-Bell, Inc.
- [41] E. Aguilar, M. Brunet, Seasonal patterns of air surface temperature and pressure change in different regions of antarctica, in: M. B. India, D. L. Bonillo (Eds.), Detecting and Modelling Regional Climate Change, Springer, pp. 215–228. doi:10.1007/978-3-662-04313-4_19.
 URL https://doi.org/10.1007/978-3-662-04313-4_19
- [42] J. G. Powers, J. B. Klemp, W. C. Skamarock, C. A. Davis, J. Dudhia, D. O. Gill, J. L. Coen, D. J. Gochis, R. Ahmadov, S. E. Peckham, G. A. Grell, J. Michalakes, S. Trahan, S. G. Benjamin, C. R. Alexander, G. J. Dimego, W. Wang, C. S. Schwartz, G. S. Romine, Z. Liu, C. Snyder, F. Chen, M. J. Barlage, W. Yu, M. G. Duda, The weather research and forecasting model: Overview, system efforts, and future directions 98 (8) 1717–1737, publisher: American Meteorological Society Section: Bulletin of the American Meteorological Society. doi:10.1175/BAMS-D-15-00308.1.
 URL <https://journals.ametsoc.org/view/journals/bams/98/8/bams-d-15-00308.1.xml>
- [43] H. Jaeger, Harnessing nonlinearity: Predicting chaotic systems and saving energy in wireless communication 304 (5667) 78–80. doi:10.1126/science.1091277.
 URL <https://www.sciencemag.org/lookup/doi/10.1126/science.1091277>
- [44] M. Lukoševičius, H. Jaeger, Reservoir computing approaches to recurrent neural network training 3 (3) 127–149. doi:10.1016/j.cosrev.2009.03.005.
 URL <http://www.sciencedirect.com/science/article/pii/S1574013709000173>
- [45] J. Garland, R. James, E. Bradley, Model-free quantification of time-series predictability 90 (5) 052910, publisher: American Physical Society. doi:10.1103/PhysRevE.90.052910.
 URL <https://link.aps.org/doi/10.1103/PhysRevE.90.052910>
- [46] T. E. Baker, A. S. Epiney, C. Rabiti, E. Shittu, Optimal sizing of flexible nuclear hybrid energy system components considering wind volatility 212 498–508.
- [47] H. E. Garcia, J. Chen, J. S. Kim, R. B. Vilim, W. R. Binder, S. M. Bragg Sitton, R. D. Boardman, M. G. McKellar, C. J. J. Paredis, Dynamic performance analysis of two regional nuclear hybrid energy systems 107 234–258. doi:10.1016/j.energy.2016.03.128.
 URL <http://www.sciencedirect.com/science/article/pii/S0360544216303759>